

The Effect of Fraction of Mill Critical Speed on Kinetic Breakage Parameters of Clinker and Limestone in a Laboratory Ball Mill

V. Deniz, A. Gelir & A. Demir

Mining Engineering Department, University of Süleyman Demirci, Isparta, Türkiye

ABSTRACT: In this study, the effect of fraction of mill critical speed was investigated on the limestone and the clinker samples using Göltaş cement factory (Isparta/Turkey) at batch grinding conditions based on a kinetic model. For this purpose, firstly, six different mono-size fractions were carried out between 0.850 mm and 0.106 mm formed by a V2 sieve series. Then, S_m and B_m equations were determined from the size distributions at different grinding times, and the model parameters (S_m , a-i.a.y and f_j) were compared for five different mill speed (fractional of mill critical speed; 55%, 65%, 75%, 85% and 95%).

The result of tests, the effect of fraction of mill critical speed on the grinding, it was found more different results from two different samples.

I INTRODUCTION

Comminution is extremely energy intensive, consuming 3% to 4% of the electricity generated world-wide, and comprising up to 70% of all energy required in a typical cement plant. Considering these factors, a small gain in comminution efficiency can have a large impact on the operating cost of a plant, while conserving resource as well (Fuerstenau et al., 1999).

During the last decade there have been considerable improvements in comminution efficiency not only due to the development of machines with the ability to enhance energy utilisation, but also due to the optimal design of grinding systems and operating variables that enable more efficient use of existing machines (Öner, 1999).

In the design of grinding circuits in cement plant, the Bond method is widely used to evaluate the performance and determine the power required and mill size for a material. This method is very complex and time consuming. In addition, it is very sensitive to procedural errors. For this reason, different methods have been proposed as alternative to the Bond method by many investigators.

In the recent years, matrix model and kinetic model, which are suggested by investigators, have been used to in the laboratory and in the industrial areas. Kinetic model, which an alternative approach is, consider comminution as a continuous process in which the rate of breakage of particles size is proportional to the mass present in that size.

The analysis of size reduction in tumbling ball mills using the concepts of specific rate of breakage and primary daughter fragment distributions has received considerable attention in years. Austin has reviewed the advantages of this approach and the scale-up of laboratory data to full-scale mills have also been discussed in a number of papers (Austin et al., 1981).

The use of Portland limestone cements has many benefits, both technical and economical. The European Pre-standard prEN 197-1 identifies 2 types of Portland limestone cement containing 6-20% limestone and 21-35% limestone, respectively. It is expected that the future world production and use of Portland limestone cement will be significantly extended. These materials have different grindabilities and the individual particle size distribution of each component influences the cement hydration and finally its performance (Tsivilis et al., 1999).

Various laboratory studies, pilot plant works and full size plant observations showed that, fraction of mill critical speed which is operating variables can affect grinding efficiency at a given output fineness.

The normal specific rates of breakage vary with speed in the same way. However, the maximum in power occurs at different fractions of critical speed from one mill to another, depending on the mill diameter, the type of lifters, the ratio of ball to mill diameter, and the ball and powder filling conditions. The maximum is usually found in the range of 70 to 85% of critical speed. Within the range of speed near the maximum power draw there are relatively small changes in the normal specific breakage rates

with rotational speed. There is no significant variation in B values with rotational speed within this range (Austin et al., 1984).

This change from cascading to cataracting pattern is the cause of the peak of feed size specific rate of breakage S, in Figure 1. In this case, J= 0.5 and U= 1 in dry batch grinding of dolomite (Herbst, and Fuerstenau, 1972). For these conditions, and with the eight 0.25 inch lifter bars on the 10 inch diameter shell, the change occurred at N=0.75. Further, the change to cataracting is accompanied by a reduction in Si and hence cascading is the major action within the mill for the conditions stated.

Austin and Brame (1983) have attempted to quantify the correction to aj in Eq. 1, and hence to S, for mill speed by:

$$a_i \propto (N - 0.1) / \{1 + \exp[15.7(N - 0.94)]\} \quad (1)$$

This paper presents a comparison of the breakage parameters with fraction of mill critical speed under the standard conditions in a small laboratory ball mill of clinker and limestone samples, which are ground at the condition 70% of critical speed of cement ball mill in Göltaş cement factory (Isparta/Turkey).

2 THEORY

When breakage is occurring in an efficient manner, the breakage of a given size fraction of material usually follows a first - order law (Austin, 1972). Thus, the breakage rate of material that is in the top size interval can be expressed as:

$$-\frac{dw_i}{dt} = S_i w_i(t) \quad (2)$$

Assuming that Si does not change with time (that is, a first-order breakage process), this equation integrates to

$$\log(w_i(t)) - \log(w_i(0)) = \frac{-S_i t}{2.3} \quad (3)$$

where, W(t) is the weight fraction of the mill hold-up that is of size i at time t and i' is the specific rate of breakage. The formula proposed by Austin et al. (1984) for the variation of the specific rate of breakage S, with particle size is

$$S_i = a_i X_i^{-\alpha} \quad (4)$$

where X_i is the upper limits of the size interval indexed by i. mm, and ai and a are model

parameters that depend on the properties of the material and the grinding conditions.

On breakage, particles of given size produce a set of primary daughter fragments, which are mixed into the bulk of the powder and then, in turn, have a probability of being refractured. The set of primary daughter fragments from breakage of size j can be represented by b_{i,j}, where b_{i,j} is the fraction of size i material, which appears in size j on primary fracture, n > i > j. It is convenient to represent these values in cumulative form.

$$B_{i,j} = \sum_{k=n}^i b_{k,j} \quad (5)$$

where, B_M is the sum fraction of material less than the upper size of size interval i' resulting from primary breakage of size y material: b_{i,y} = B_w - B₊; .. Austin et al. (1981) have shown that the values of B_{i,j} can be estimated from a size analysis of the product from short time grinding of a starting mill charge predominantly in size j (the one-size fraction B11 method). The equation used is,

$$B_{i,j} = \frac{\log[1 - P_i(t)] / \log[1 - P_i(0)]}{\log[1 - P_{i+1}(t)] / \log[1 - P_{i+1}(0)]} \quad n \geq i \geq i+1 \quad (6)$$

where, P_i(t) is the fraction by weight in the mill charge less than size X_i at lime t. B_{i,j} can be fitted to an empirical function (Austin and Luckie, 1972).

$$B_{i,j} = \phi_j [X_{i-1}/X_j]^\gamma + (1 - \phi_j) [X_{i-1}/X_j]^\beta \quad n \geq i \geq j \quad (7)$$

where

$$\phi_j = \phi_1 [X_j / X_1]^{-\delta} \quad (8)$$

where, δ, 0, γ, and β are model parameters that depend on the properties of the material. It is found that, B functions are the same for different ball filling ratios, mill diameters, etc. (Austin et al., 1984). If B_{i,j} values are independent of the initial size, i.e. dimensionally normalizable, then S is zero.

3 EXPERIMENTAL STUDIES

3.1 Materiell

Limestone and clinker samples taken from Göltaş cement factory (Isparta/Turkey) were used as the experimental materials. The chemical properties of the limestone and the clinker samples are presented in Table I.

3.2 Grinding Tests

Firstly, Standard Bond Work index tests were made for limestone and clinker samples. The Bond Work

index values of limestone and clinker samples were determined as 13.52 kWh/t and 13.69 kWh/t, respectively. The standard set of grinding conditions used is shown in Table 2, for a laboratory mill 6283 cm volume. Six mono-size fractions (-0.850+0.600, -0.600+0.425, - 0.425 +0.300, - 0.300+ 0.212, - 0.212+0.150, -0.150+0.106 mm) were prepared and ground batch wise in a laboratory-scale ball mill for determination of the breakage functions. Each sample was taken out of the mill and dry sieved for product size analysis.

Table I. Chemical composites of clinker and limestone samples using in experiments.

Oxides (t/t)	Limestone	Clinker
SiO ₂	10.60	22.22
Al ₂ O ₃	1.07	3.61
Fe ₂ O ₃	0.59	3.30
CaO	48.99	67.44
MgO	1.11	1.80
SO ₃		1.50
Loss on ignition	38.72	0.11

Table 2. The standard set of grinding conditions.

Mill	Diameter, mm	200				
	Length, mm	200				
	Volume, cm ³	6283				
Mill	Critical (N _c), rpm	101				
Speed	Operational (φ _c), %	55	65	75	85	95
Balls	Diameter, mm	25.4				
	Specific gravity	7.8				
	Quality	Alloy Steel				
	Assumed porosity, %	40				
Material	Ball filling volume fraction (J%) ^b	20				
	Specific gravity	Clinker: 3.0		Limestone: 2.69		
	Powder filling volume fraction (f _v %) ^c	4.2				
	Interstitial filling (U%) ^d	52.5				

^a Calculated from $N = 42 \sqrt{\sqrt{D} - d}$ (D, d in metres)

^b Calculated from $J = \left(\frac{\text{mass of balls} \times \text{ball density}}{\text{mill volume}} \right) \times \frac{100}{\rho_s}$

^c Calculated from $f = \left(\frac{\text{mass of powder} \times \text{powder bulk density}}{\text{mill volume}} \right)$

^d Calculated from $U = \frac{J}{4f}$

4 RESULTS AND DISCUSSION

4.1 Determination of S parameters

The first-order plots for the various feed sizes of limestone and clinker samples are given in Figure 2 to 1. The results indicated that breakage generally the first-order relation and values of S, could be determined from the slope of straight-line of first-order plots (Table 3 to 4). Additional, Figure 12 to 13 shows the values of S, for grinding of the five fraction of mill critical speed studied, as a function of size.

4.2 Determination of B parameters

The values of B were determined from the size distributions at short grinding times using BII method, and arc shown in Figure 14 to 15. The results of limestone and clinker samples showed a typical normalized behaviour, so that the progeny distribution did not depend on the feed particle size and the parameter B was zero. The model parameters are also given in Table 3- 4.

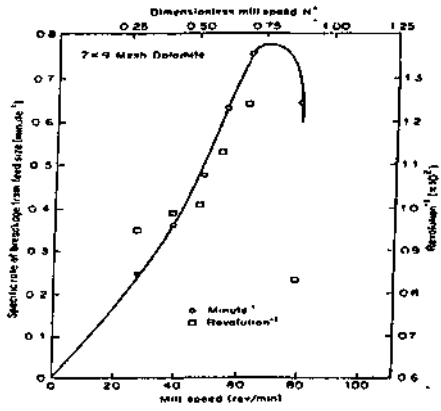


Figure 1. Variation of specific rate of breakage from feed size versus mill speed (Herbst and Fuerstenau, 1972).

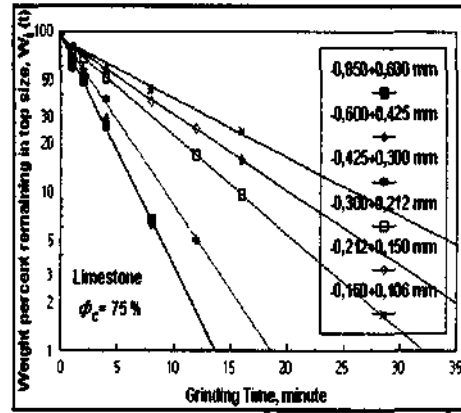


Figure 4. First-order plots for $\phi_c = 75\%$ of Limestone.

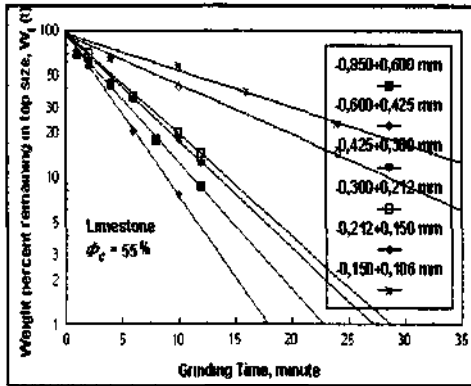


Figure 2. First-order plots for $\phi_c = 55\%$ of Limestone.

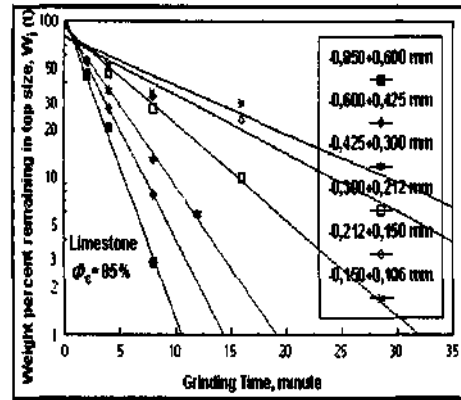


Figure 5. First-order plots for $\phi_c = 85\%$ of Limestone.

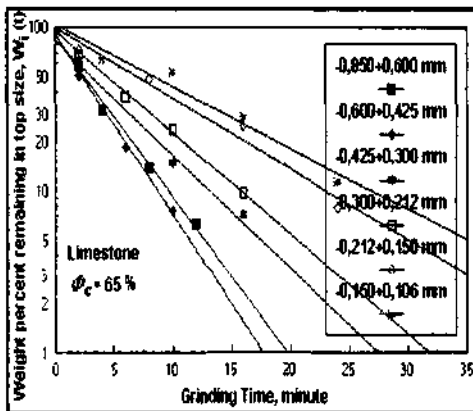


Figure J. First-order plots for $\phi_c = 65\%$ of Limestone.

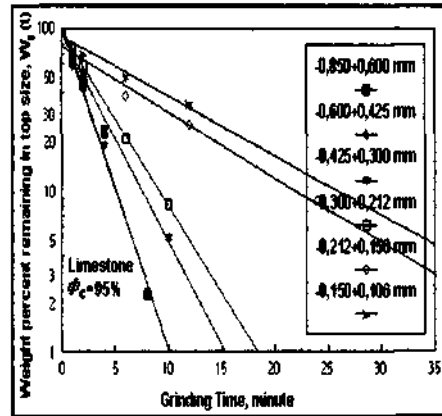


Figure 6. First-order plots for $\phi_c = 95\%$ of Clinker.

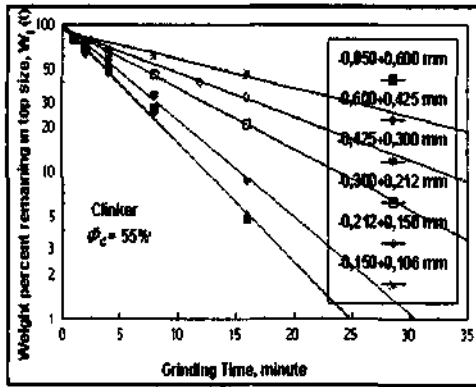


Figure 7 First-order plots for $\phi_c = 55\%$ of Clinker

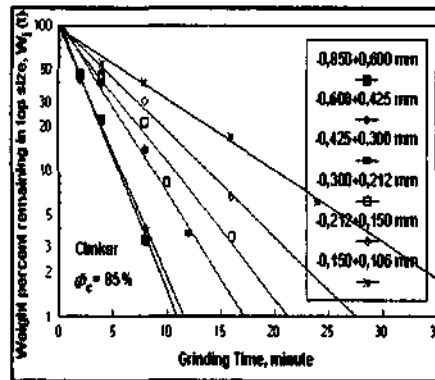


Figure 10 First-order plots for $\phi_c = 85\%$ of Clinker.

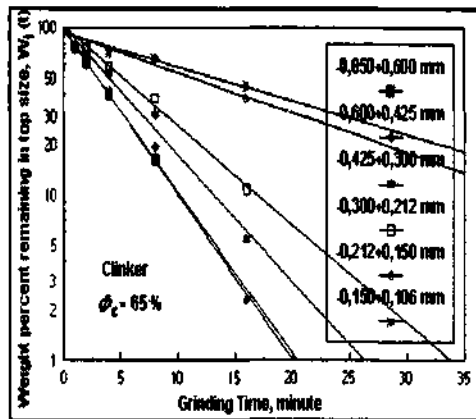


Figure 8. First-order plots for $\phi_c = 65\%$ of Clinker.

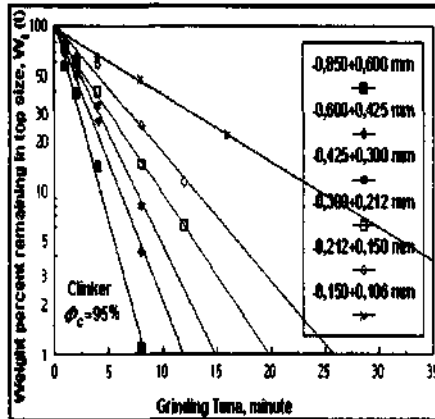


Figure 11. First-order plots for $\phi_c = 95\%$ of Clinker.

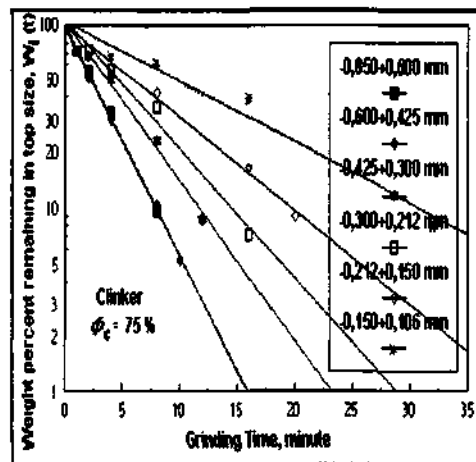


Figure 9. First-order plots for $\phi_c = 75\%$ of Clinker.

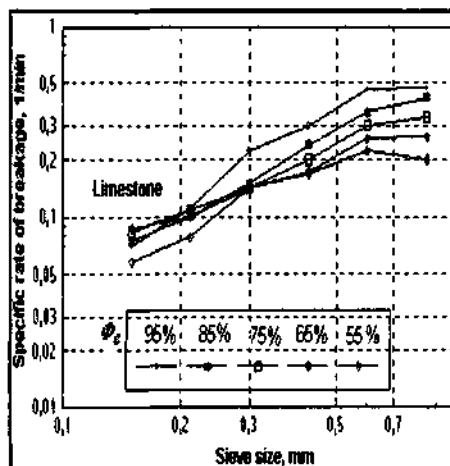


Figure 12 Specific rates of breakage for Limestone

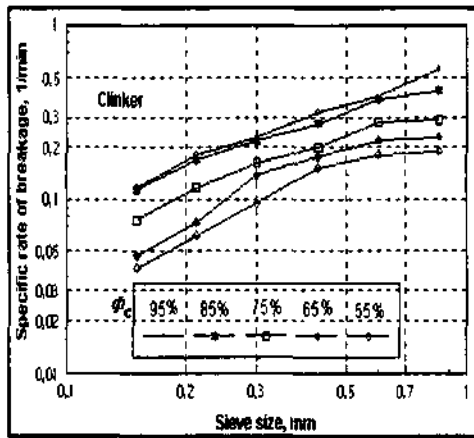


Figure 13. Specific rates of breakage for Clinker.

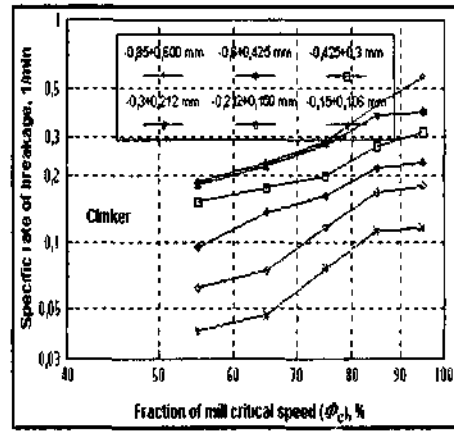


Figure 16 Variation of specific rate of breakage with fraction of critical mill speed for Limestone.

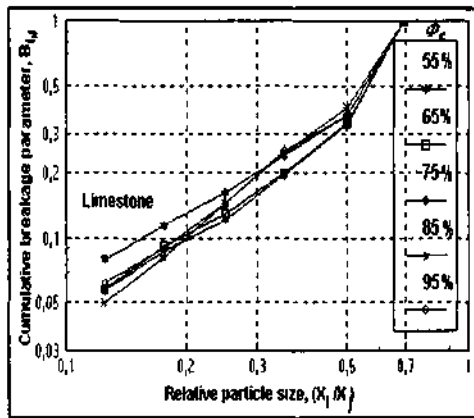


Figure 14. Cumulative breakage distribution functions for Limestone.

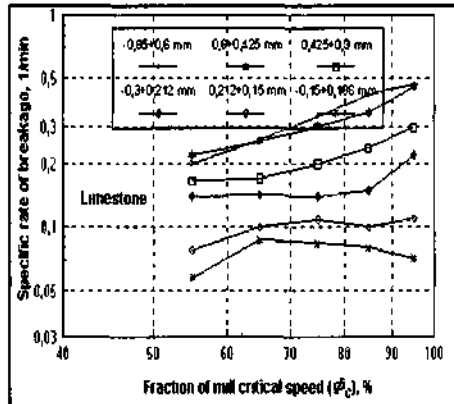


Figure 17. Variation of specific rate of breakage with fraction of critical mill speed for Clinker.

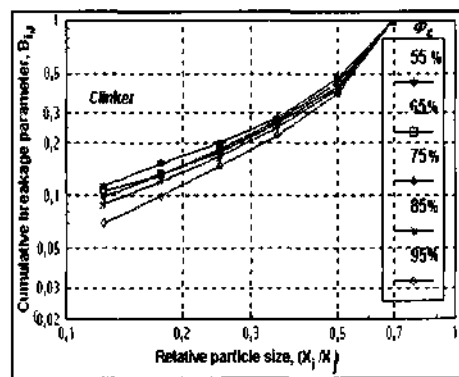


Figure 15 Cumulative breakage distribution functions for Clinker

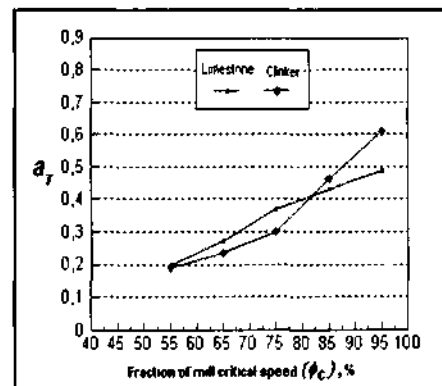


Figure 18 Variation of a_T with fraction of critical mill speed.

Table 3. Model parameter values of limestone for fraction of mill critical speed.

ϕ (%)	$0.300+0.212$ (mm) Si	α	a_T	ϕ_1	γ
55	0.139	0.831	0.199	0.507	1.315
65	0.141	0.765	0.273	0.510	1.336
75	0.142	0.752	0.371	0.514	1.357
85	0.150	0.833	0.436	0.504	1.432
95	0.220	1.278	0.489	0.497	1.237

Table 4. Model parameter values of clinker for fraction of mill critical speed.

(%)	$0.300+0.212$ (mm) Si	a	a_T	$\langle \phi \rangle$	γ
55	0.095	1.261	0.191	0.419	0.801
65	0.137	1.314	0.234	0.415	0.809
75	0.162	1.249	0.301	0.413	0.848
85	0.217	1.241	0.462	0.394	0.857
95	0.230	1.272	0.611	0.387	1.081

It can be seen from the data in Table 3-4 that model parameter values with the fraction of mill critical speed is similar to that indicated by the critical speed, with the ϕ values, showing the trend to decrease for both samples, and the γ values to increase with the increase in traction of mill critical speed for clinker, but γ values to increase with the increase up to 85% of mill critical speed for limestone, later γ values to decrease for higher from 85% of mill critical speed. The maximum of γ is usually found in 85% of mill critical.

4.3 Variation of specific rate of breakage with fraction of mill critical speed

Herbst and Fuerstenau (1972) demonstrated relationships of specific rate of breakage from feed size versus mill speed. For this same purposes, variation of specific rate of breakage with fraction of mill critical speed for limestone and clinker samples were investigated, and show the graphical represent Figure 16 to 17.

The result of graphical representation, it was found different results than Herbst and Fuerstenau (1972).

4.4 Variation of a_T values with fraction of mill critical speed

Austin and Brame (1983) showed variation of a_T with mill speed in Eq. 1. For this purpose, variation of a_T values with fraction of mill critical speed for both samples were investigated, and show the graphical represent Figure 18. Eq. 9, 10 for clinker and limestone could be determined from Figure 18. The functions of this present work are different from Eq.1.

For Clinker;

$$a_T = 0,0344 \exp(0,003\phi_i) \quad r^2 = 0.98$$

For Limestone;

$$a_T = 0,0225 \exp(0,062\phi_i) \quad r^2 = 0.96 \quad (10)$$

5 CONCLUSIONS

The dry grinding of size intervals of limestone and clinker samples showed that both samples followed the first-order breakage law with constant normalised primary breakage distributions. In addition, these samples do not depend on the particle size from cumulative breakage distribution function.

Although, limestone and clinker samples have close work index values 13.53 kwh/t and 13.69 kwh/t, respectively, they have demonstrated different characteristics entirely in the selection function and the breakage function model parameters.

The values of the primary daughter fragment distributions and the values of a in $S_i = a_j X_i^a$ were difference in the limestone and the clinker. As the amount of S_i , or a_j values increased, the effective breakage increase, and broke as very fast in the undersize of original particle size. The experimental values show that a_T grinding is faster grinding for every two samples as fraction of mill critical speed increase. But, clinker is faster grinding of original particle size than limestone.

Herbst and Fuerstenau (1972) showed that change from cascading to cataracting pattern is the cause of peak of feed size specific rate of breakage S_i , the change occurred at $\langle \phi \rangle = 75\%$. The present study showed that change from cascading to cataracting pattern is occurred at $\langle \phi \rangle = 85\%$.

Austin et al. (1984) demonstrated that variation B values are no significant with rotational speed. The present work is significant variation B values with fraction of mill critical speed.

The B_i values for grinding of clinker are different from the B_i values of limestone, since the ground materials are different from each other. The γ value of clinker is lower than that of limestone ($\gamma =$ from 0.801 to 1.081 for clinker, $\gamma =$ from 1.231 to 1.431 for limestone), which emphasizing that the grinding of clinker produces more fine material in the fines region than the limestone grinding.

$\langle \phi \rangle$ values of clinker samples have decreased with increasing fraction of mill critical speed. However, ϕ_1 values of limestone sample have decreased value up to 75% with increasing fraction of mill critical speed and it researches to peak point and, ϕ_i values have decreased for later 75% mill critical speed.

In this study, it has been appeared that, these experimental values for every sample must be seen in order to lower the energy costs in grinding process.

REFERENCES

- Austin. L.G.. 1972. A review introduction to the description of grinding as a rate process. *Powder Technology*. Vol. 5. 1-7.
- Austin. L.G. and Luckie. P.T.. 1972. Methods for determination of breakage distribution parameters. *Powder Technology*. Vol. 5. 215-222.
- Austin. L.G. and Bagga. R., Çelik. M.. 1981. Breakage properties of some materials in a laboratory ball mill. *Powder Technology*. Vol.28. 235-241
- Austin. L.G. and Brame. K.. 1983. A comparison of the Bond method for sizing wet tumbling mills with a size-mass balance simulation method. *Powder Technology*. Vol. 34. 261-274.
- Austin, L.G., Khmpel. R.R. and Luckie. P.T. (eds.). 1984. *Process Engineering of Size Reduction: Ball Milling*. A.I.M.E., S.M.E., NewYork, USA.
- Fuerslenau. D.W., Lutch. J.J. and De. A.. 1999. The Effect of ball size on the energy efficiency of hybrid-pressure toll mill/ball mill grinding. *Powder Technology*. Vol.105. 199-204.
- Herbst. I.A. and Fuerslenau. D.W.. 1972. Influence of mill speed and ball loading on the parameters of batch grinding equation. *Trans. SME/AIME*. Vol. 252. 169-176.
- Öner. M.. 1999. Ball size rationing affects clinker grinding. *World Cement Research*. February. 101-106.
- Tsivilis. S., Voglis. N. and Photou. J.. 1999. A study on the intergrinding of clinker and limestone. *Mineral Engineering*. Vol. 12. 837-840.